

# THE ELECTRICAL RESISTIVITY OF CYTOPLASM

KENNETH R. FOSTER, JEANNETTE M. BIDINGER,  
and DAVID O. CARPENTER

*From the Neurobiology Department, Armed Forces Radiobiology Research Institute, Bethesda, Maryland 20014. Dr. Foster's present address is Department of Bioengineering, University of Pennsylvania, Philadelphia, Pennsylvania 19174*

**ABSTRACT** The apparent cytoplasmic resistivity of two different giant cells has been measured using an extension of a previously developed single microelectrode technique. Each cell is penetrated by a metal microelectrode whose complex impedance is measured as a function of frequency between 500 kHz and 5.7 MHz. By plotting the measured impedance data on the complex  $Z$  plane and extrapolating the data to infinite frequency, the substantial effects of electrode polarization can be overcome. For *Aplysia* giant neurons and muscle fibers of the giant barnacle, the extrapolated cytoplasmic specific resistivities are 40 and 74  $\Omega$ -cm, respectively, at infinite frequency. The barnacle data are in excellent agreement with sarcoplasmic resistivity values derived from the measured cable properties of other marine organisms, and from high frequency conductivity cell measurements in intact barnacle muscle tissue.

In the *Aplysia* neurons, the frequency-dependent part of the electrode impedance is larger when the electrode is in a cell than when it is in an electrolyte solution with the same specific resistivity as the aqueous cytoplasm; however, the phase angle of the frequency-dependent component of the electrode impedance is the same in both cases. This suggests that the high apparent values of cytoplasmic resistivity found using the single microelectrode technique at lower frequencies probably reflect an artifact caused by reduction of the effective surface area of the electrode by intracellular membranes, with a corresponding increase in its polarization impedance.

## INTRODUCTION

Many previous studies have shown that the electrical resistivity of the aqueous cytoplasm of most cells is two to three times that of the extracellular fluid. These estimates have resulted primarily from cable studies on nerve axons (1) or muscle fibers (2-6), or from dielectric measurements on suspensions of cells (7). Although nerve cell bodies cannot be studied using these techniques, their cytoplasmic resistivities are normally assumed to be equal to that of axoplasm. The chief motivation for this study has been to find the underlying reasons for the extraordinarily high apparent intracellular resistivity in the nerve cell bodies of the sea slug *Aplysia californica*, found to be about one-twentieth that of the surrounding seawater in previous studies by this laboratory (8, 9). It was suggested that this high resistivity might result from unusually

low ionic mobilities in these cells, perhaps indicating an unusual degree of ion binding or water structure in these cells. In this study, we reexamine those findings.

As in the previous studies, we have used a single metal electrode, which is well insulated except for a small area near its tip, to measure the cytoplasmic resistivity. The AC impedance of this electrode is assumed to be a function of the resistivity of the electrolyte in the immediate vicinity of its tip, and that the measurement frequency ( $>500$  kHz) is sufficiently great that cell membranes are effectively shorted out. Even at these high frequencies, the electrodes we used all polarized significantly, complicating the interpretation of the impedance data. One approach (used in the previous studies) is to ignore these effects, assuming that the polarization impedance of the electrode is a function only of the resistivity of the electrolyte, regardless of its ionic composition. A recent study of polarization effects in gold electrodes (10), and control experiments using platinum electrodes in various electrolyte and concentrated protein solutions (9), support this assumption. Using the microelectrode technique, the resistivity of squid axoplasm was found to be  $31 \Omega\text{-cm}$  (11), in good agreement with more conventional measurements (1, 12), further justifying this assumption. On the other hand, Schwan (13) has shown that the polarization impedance of large platinum electrodes increases in the presence of cell membranes, perhaps because their effective area is reduced by membranes adjacent to the metal surfaces. This observation, if correct, would predict serious artifacts in the previous intracellular impedance measurements (8, 9). The previous studies, which employed relatively low frequencies ( $\leq 100$  kHz), have been expanded here to include measurements of the complex microelectrode impedance over the frequency range 500 kHz to 5.7 MHz. We attempt to distinguish the (frequency-dependent) polarization impedance from the (frequency-independent) electrode spreading resistance due to electrolyte resistance to current flow from the electrode tip. In order to test our technique, we have also measured the apparent cytoplasmic resistivity of single muscle fibers of the barnacle, *Balanus nubilus*. While cable constants for these fibers are apparently not available in the literature, cytoplasmic resistivities of the large muscle fibers of the marine crabs *Carcinus maenas* and *Portunus depurator* are known to be about  $69 \Omega\text{-cm}$  (3). In addition, the resistivity of the barnacle muscle tissue can be measured using conventional dielectric techniques at a sufficiently high frequency (10–100 MHz) that effects of the cellular membranes should be negligible in these measurements as well, providing an independent means of estimating the resistivity of the sarcoplasm.

We will show that, for both tissues studied, the cytoplasmic resistivity, obtained by extrapolating the electrode impedance data to infinite frequency to overcome electrode polarization effects, is within the range of values reported in (1–7), and does not differ from that of the external seawater by more than a factor of four.

## METHODS

All impedance measurements reported here were performed using an active RF vector impedance meter (Model 4815A, Hewlett-Packard Corp., Palo Alto, Calif.). This instrument injects a constant RF current of  $2 \mu\text{A}$  into a probe located a few centimeters from the metal electrode;

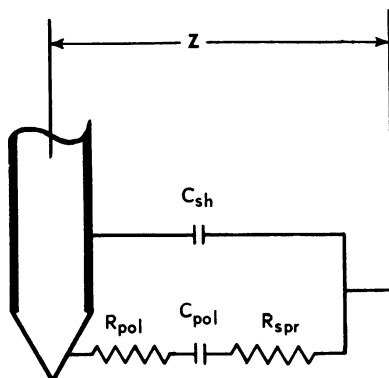


FIGURE 1 An equivalent circuit for the polarizable microelectrode, bath, and the (nonpolarizable) indifferent electrode. The polarization impedance of the metal electrode is represented by a capacitance  $C_{pol}$  in series with a resistance  $R_{pol}$ , where both of these parameters depend upon the frequency and other variables. A small capacitance  $C_{sh}$  between the insulated electrode shaft and the bath can be separately measured and subtracted from the data; the spreading resistance,  $R_{spr}$ , to the current flow through the electrolyte solution near the tip of the electrode is proportional to the solution resistivity, and (we assume), to the cytoplasmic resistivity as well.

from the measured RF voltage at the probe, it then calculates the complex impedance  $Z$  between the probe terminal and ground. Of particular importance for this study, the measurement frequency can be continually varied, allowing rapid measurements on an undisturbed preparation.

The approximate electrical equivalent of the circuit consisting of the metal microelectrode, electrolyte bath, and grounded extracellular reference electrode is shown in Fig. 1. The ground electrode was a well-platinized platinum plate of  $5.0 \text{ cm}^2$  surface area, whose polarization impedance was negligible at all frequencies used in this study; it consequently does not appear in Fig. 1.

Possible effects of lead inductance are not considered in this circuit. Because of the short leads ( $<10 \text{ cm}$  total length), low residual inductance of the probe ( $\sim 8 \text{ nH}$ ), and high electrode impedance ( $>1 \text{ k}\Omega$ ), such effects were apparently negligible over the entire frequency range of the instrument, 0.5 to 108 MHz.

The electrode spreading resistance ( $R_{spr}$ ) due to the electrolyte resistivity is the quantity we wish to determine. For a hypothetical spherical electrode of radius  $r$  immersed in an infinite electrolyte solution of specific resistivity  $\rho \text{ }\Omega\text{-cm}$ ,

$$R_{spr} = \rho / 4\pi r. \quad (1)$$

Simple calculations show that in this case 75% of the total electrode spreading resistance occurs within a distance  $4r$  from the electrode center. The observed proportionality between  $R_{spr}$  and the solution resistivity is a useful check on the accuracy of our analysis.

Because it cannot be nulled out as with a conventional impedance bridge, the shunt capacitance  $C_{sh}$  between the active probe terminal and ground becomes the chief limitation to the resolution of the electrode impedance measurements at high frequencies. Much of this capacitance ( $\sim 1.0 \text{ pF}$ ) occurs within the probe itself, and is constant. The leads and microelectrode shaft contribute an additional picofarad or so, which is also constant provided the position of the leads is not changed during a measurement and provided the electrode is immersed to the same depth each time in the seawater or in the KCl solutions used to calibrate the electrode. The total stray capacitance can be measured in two ways. During the calibration procedure

$C_{sh}$  can be accurately measured by replacing the electrolyte calibrating solution with de-ionized water; the electrode then behaves as a pure capacitance whose value is  $C_{sh}$ . When the electrode tip is inside a cell, tissue near the electrode shaft increases the effective dielectric constant of the electrolyte, increasing  $C_{sh}$  by about 0.7 pF. In this case,  $C_{sh}$  can be better estimated by raising the measurement frequency until the (frequency-dependent) polarization impedance becomes negligible. We have found that the electrode capacitance is generally constant above 50 MHz, and that in the calibrating solutions these two techniques give values of  $C_{sh}$  which agree to within 0.2 pF. Above 5 MHz, the admittance of  $C_{sh}$  becomes significant compared to the electrode admittance, making estimates of the remaining circuit parameters increasingly uncertain.

Unlike the previous studies in this series, we consider the electrode polarization impedance,  $Z_{pol}$ , to be an artifact which must be excluded from the measurements. This impedance can be described as a resistance,  $R_{pol}$ , in series with a capacitance,  $C_{pol}$ , both of which vary with frequency ( $f$ ), solution resistivity, electrode surface area, and perhaps other variables. Robinson (14) describes the polarization effects found with metal microelectrodes similar to those employed here. While the detailed molecular mechanisms of this polarization impedance are unknown, the variation of  $Z_{pol}$  with frequency has been well studied (15). Given:

$$Z_{pol} = R_{pol} - j/2\pi f C_{pol}$$

$$j = \sqrt{-1},$$

the phase angle of  $Z_{pol}$  is usually observed to be constant, independent of frequency:

$$\tan^{-1}(1/2\pi f C_{pol} R_{pol}) = \alpha\pi/2. \quad (2)$$

Further, the magnitude of  $Z_{pol}$  can be empirically described by a simple power function of  $f$  which is valid over many decades of frequency:

$$R_{pol} \propto f^{-\alpha}$$

and

$$|Z_{pol}| \propto f^{-\alpha}. \quad (3)$$

Note that the parameter  $\alpha$  is the same as that defined in Eq. 2. Agreement between our calculated electrode impedance data and the empirical Eqs. 2 and 3 is an additional check on our results. After correction for  $C_{sh}$ , the total impedance of the electrode is thus  $R_{spr} + Z_{pol}$ , plus (presumably negligible) contributions from the cell membrane. If the imaginary part of this impedance is plotted vs. its real part, the data (from Eq. 2) will be described by a straight line which intersects the real axis at  $R_{spr}$  at an angle  $\alpha\pi/2$  (radians).

The glass-insulated platinum microelectrodes were similar in construction, but considerably larger, than those used in the previous studies (8, 9). Their exposed tips had been electrolytically sharpened into cones, 5–10  $\mu\text{m}$  tip diameter increasing to about 20  $\mu\text{m}$  in diameter at the start of the insulation, and generally 40–50  $\mu\text{m}$  in length. The effective diameter of the electrodes, determined from the calibration data and Eq. 1, was about 40  $\mu\text{m}$ . They were platinized by dipping them into a 3% platinum chloride solution containing 0.025% lead acetate, and passing a constant current of 1  $\mu\text{A}$  for 15 s, with two changes of polarity. The size of acceptable electrodes is narrowly limited by the size of the cell to be penetrated ( $\sim 500 \mu\text{m}$  for the large *Aplysia* neurons) and by the need to maximize the exposed electrode surface area to reduce polarization effects. Electrodes much smaller than those employed here polarized so badly that the high frequency data could not be extrapolated to determine  $R_{spr}$ .

During each experiment the electrode was clamped firmly in a plastic jig and held by a conventional micromanipulator above the calibration solutions or tissue preparation. The Lucite

sample chamber and all the leads were kept well away from the metal table surface, to prevent eddy currents which lead to stray inductance. Before penetration of each cell, the electrode was calibrated using KCl solutions of known resistivity. The reference and microelectrodes were then washed with distilled water and the specimen chamber placed before the micromanipulator. The cells had been dissected from the animals, freed of connective tissue, and pinned to a layer of Sylgard (Dow Corning, Midland, Mich.) in the chamber. Cell membrane potentials were measured using a conventional glass microelectrode. Cells were not studied if they had electrical parameters indicating injury (resting potentials less than  $-40$  or  $-60$  mV for *Aplysia* neurons and barnacle muscle fibers, respectively). Each *Aplysia* neuron (most often the R2 cell from the abdominal ganglion) was  $500\text{--}1000\ \mu\text{m}$  across; the fibers from the barnacle adductor muscle averaged  $1000\ \mu\text{m}$  in diameter. The cells were penetrated by the metal microelectrode with the help of a dissecting microscope. As the electrode penetrated the cell, its impedance abruptly increased and remained constant upon deeper penetration. Within 5 min after penetration, electrode impedance measurements had been performed at eight frequencies between 0.5 and 5.7 MHz, and at five frequencies between 32 and 100 MHz. As explained above, these latter measurements were used to estimate the total stray capacitance of the circuit. There was no evident drift in the electrode impedance during this interval. The membrane potential of the cell was measured after removal of the metal electrode, and the electrode was recalibrated. A significant change in the electrode calibration data usually indicated mechanical injury to the electrode; these experiments were discarded. Upon withdrawal of the metal electrode, the *Aplysia* membrane potentials had often fallen by about 20 mV, indicating membrane damage; the barnacle muscle fibers were more resistant to damage. During the measurements, the cells were barely covered with artificial seawater ("Instant Ocean"). All measurements were performed at room temperature ( $20^\circ\text{C} \pm 1^\circ\text{C}$ ).

As an additional check on the barnacle data, blotted muscle tissue was packed into a standard conductivity cell whose resistance was measured using the vector impedance meter. The specific resistance of the tissue was calculated after correcting these measurements for the residual series inductance of the cell ( $\sim 60$  nH) using the standard formula (13).

## RESULTS

The data from a typical experiment on a barnacle muscle fiber are shown in Fig. 2. In each of the four sets of data (i.e., the three calibration runs in KCl and the experiment in the cell), the frequencies range from 0.5 to 5.7 MHz, increasing by a factor of 1.4 for each step. In this experiment, the stray capacitance  $C_{\text{sh}}$  is 2.0 pF and 2.8 pF, for the electrode immersed to the same depth in the calibrating solutions and in the cell, respectively. Since the stray capacitance with the electrode just above the electrolyte bath is 1.2 pF, the apparent dielectric constant of this barnacle fiber is  $\sim 160$  in the range 10 to 100 MHz, in agreement with literature values (13) for (mammalian) muscle tissue. Both in the fiber and in the calibration solutions, the electrode impedance is complex and frequency-dependent, evidently due to polarization effects in both cases. The extrapolated spreading resistance is proportional to the solution resistivity (Fig. 2, inset), as expected. The cell in Fig. 2 has an apparent resistivity of  $110\ \Omega\text{-cm}$ , with the other barnacle cells ranging between 20 and  $95\ \Omega\text{-cm}$  (Table I). Excluding experiment 3, (where possibly the electrode tip was accidentally pushed through the cell and into the seawater below), the average resistivity of these fibers is  $82 \pm 21\ \Omega\text{-cm}$ . The observed polarization phase angle,  $\alpha\pi/2$ , is 10–20% larger than

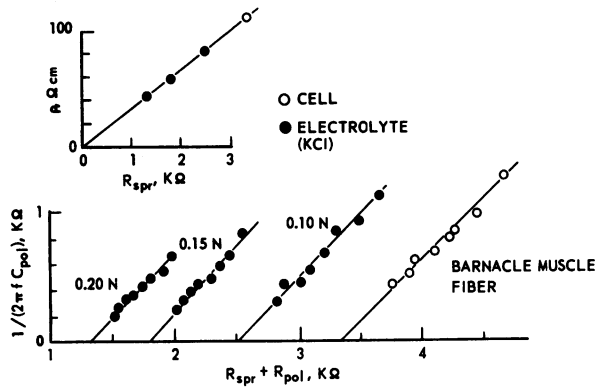


FIGURE 2 A typical set of experimental data from a single muscle fiber of the barnacle. The complex electrode impedance is shown as a function of frequency, when it is in calibrating solutions of KCl and after it has penetrated the cell. The measurement frequencies range from 0.5 to 5.7 MHz, in equal logarithmic steps. The frequency-dependent part of the measured impedance arises from electrode polarization, both when the electrode is in the electrolyte and (apparently) when it is in the cell. The frequency-independent component of the electrode impedance,  $R_{spr}$ , is proportional to the solution resistivity,  $\rho$  (inset). This cell has an apparent sarcoplasmic resistivity of 110  $\Omega$ -cm, at 20°C.

that calculated from the frequency dependence of  $Z_{pol}$ , possibly indicating a minor systematic error in the measurements (see below). The conductivity cell measurements on one tissue sample at 23–25°C are presented in Fig. 3, with literature values for the specific resistivity of lysed, packed bovine erythrocytes (25°C) (16) shown for comparison. Both samples had the same average water content (65–75% by weight). The 2.5-fold higher resistivity of the erythrocyte cytoplasm is primarily due to the lower ionic

TABLE I  
IMPEDANCE DATA FROM GIANT BARNACLE  
MUSCLE FIBERS (20°C)

Experiment	$\rho$	$\alpha$ (from phase angle of $Z_{pol}$ )	$\alpha$ (from frequency dependence of $R_{pol}$ )
	$\Omega$ -cm		
1	110	0.460	0.407
2	95	0.369	0.300
3	25	0.277	0.300
4	86	0.355	0.274
5	55	0.401	0.308
6	88	0.323	0.245
7	60	0.216	0.170

Average  $\rho = 74.1 \pm 29.0 \Omega$ -cm.

Excluding Exp. 3,  $\rho = 82.3 \pm 21.0 \Omega$ -cm.

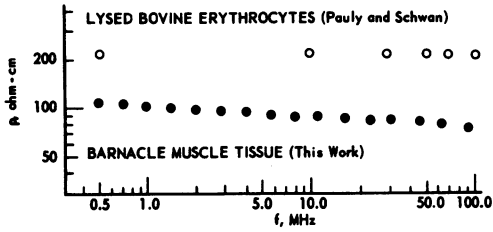


FIGURE 3

FIGURE 3 The resistivity of intact barnacle depressor muscle tissue, measured using a conventional conductivity cell with platinum electrodes, at 23–25°C. The tissue had been blotted on filter paper after removal from the animal, and samples of about 1 cm<sup>3</sup> volume packed into the cell. At frequencies above 10 MHz, the resistivity of this tissue is approximately constant, 85 Ω-cm for this sample. Also shown is the specific resistivity of lysed, packed bovine erythrocytes at 25°C (from reference 18), a preparation which contains roughly the same protein concentration as the barnacle fibers. The 2.5-fold higher resistivity of the lysed erythrocytes primarily results from the lower ionic strength of mammalian plasma.

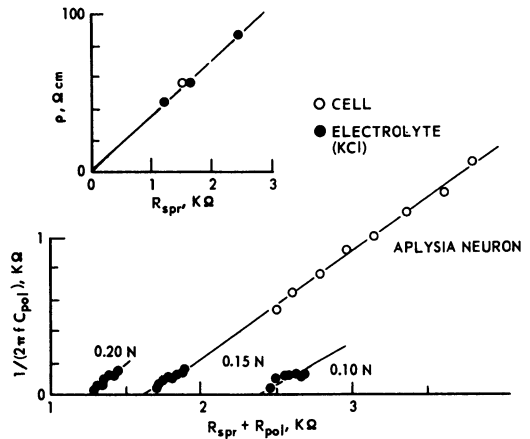


FIGURE 4

FIGURE 4 A typical set of experimental data from an *Aplysia* neuron (cell R2, right abdominal ganglion). In this preparation, (as in the other experiments on *Aplysia* neurons), the electrode polarization impedance apparently increases 10-fold after penetration of the cell. By extrapolating the complex electrode impedance to the real axis, the apparent intracellular resistivity of this cell is  $61 \pm 3 \Omega\text{-cm}$ , at 20°C.

strength of mammalian plasma (300 mosmol vs. 1000 mosmol for seawater). The average resistivity of two barnacle muscle samples at several frequencies between 30 and 100 MHz is  $82.6 \pm 7.6 \text{ ohm-cm}$ , in good agreement with the microelectrode results. Resistivity values obtained from cable studies on barnacle fibers are apparently not available in the literature, but Fatt and Katz (3) found the sarcoplasmic resistivity of muscle fibers from the marine crabs *Carcinus maenas* and *Portunus depurator* to be  $69 \pm 33 \Omega\text{-cm}$ . We expect that cable studies on the barnacle muscle fibers would produce similar values for this parameter.

As evident in Fig. 2, the electrode polarization impedance in the barnacle muscle fiber is not greatly different from that in a KCl solution of similar resistivity. When an electrode penetrates an *Aplysia* neuron, in contrast, the frequency-dependent part of its impedance increases 10-fold in magnitude (Fig. 4), in agreement with the previous observations (8, 9). However, the phase angle of this impedance is the same with the electrode in the cell or in the calibration solutions of the same resistivity. This suggests that the same polarization effects determine the frequency-dependent part of the

electrode impedance when its tip is in the cell as well as in the KCl calibrating solutions. From the electrode spreading resistance, the cell in Fig. 4 has an apparent somatoplasmic resistivity of 61  $\Omega$ -cm. From twelve experiments, the average resistivity of the *Aplysia* cytoplasm is  $40 \pm 14$   $\Omega$ -cm, somewhat greater than that of squid axoplasm (27 to 31  $\Omega$ -cm) (1, 11, 12) and of seawater (20  $\Omega$ -cm).

## DISCUSSION

The precision of our results is determined by the 25–35% variance in the measured cytoplasmic resistivities (Tables I and II). The major probable source of systematic error is in the estimation of  $C_{sh}$ , and this limits the accuracy of our results. As discussed above, when the electrode is in a cell or in a KCl calibrating solution, this parameter is determined from the electrode impedance at several frequencies in the range from 30 to 100 MHz, where the electrode polarization impedance is generally negligible, and the electrode capacitance approaches a constant value. This parameter can also be determined by dipping the electrode to the same depth in deionized water, where it behaves as a pure capacitor whose value is  $C_{sh}$ . When the electrode is immersed to a constant depth in KCl solutions, these two techniques give values of  $C_{sh}$  which agree to within  $\pm 0.2$  pF. When the electrode penetrates an *Aplysia* neuron, its polarization impedance increases, and the data require considerable extrapolation to determine  $R_{spr}$ . A small systematic error in  $C_{sh}$ , therefore, can result in a much greater systematic error in the final calculated cytoplasmic resistivities. In order to explore this possibility, we calculated the spreading resistance from a typical experiment with

TABLE II  
IMPEDANCE DATA FROM *APLYSIA*  
GIANT NEURONS (20°C)

Experiment	$\rho$	$\alpha$ (from phase angle of $Z_{pol}$ )	$\alpha$ (from frequency dependence of $R_{pol}$ )
	$\Omega$ -cm		
1	48	0.354	0.351
2	11	0.281	0.200
3	35	0.341	0.319
4	43	0.363	0.331
5	47	0.335	0.368
6	50	0.433	0.359
7	26	0.231	0.178
8	61	0.409	0.401
9	46	0.453	0.424
10	26	0.265	0.234
11	37	0.378	0.360
12	59	0.261	0.274

Average  $\rho = 40.3 \pm 13.9$   $\Omega$ -cm.



TABLE III  
EFFECT OF THE STRAY CAPACITANCE  $C_{sh}$  ON THE CALCULATED  
CYTOPLASMIC RESISTIVITY\*

$C_{sh}$	$\alpha$ (from phase angle of $Z_{pol}$ )	$\alpha$ (from frequency dependence of $R_{pol}$ )	$R_{spr}$	Calculated $\rho$
<i>pF</i>			<i>k<math>\Omega</math></i>	<i><math>\Omega</math>-cm</i>
2.3	0.376 $\pm$ 0.015	0.346 $\pm$ 0.006	1.45 $\pm$ 0.08	51
2.5	0.391 $\pm$ 0.015	0.369 $\pm$ 0.008	1.58 $\pm$ 0.07	56
2.7	0.409 $\pm$ 0.016	0.401 $\pm$ 0.010	1.71 $\pm$ 0.07	61
2.9	0.414 $\pm$ 0.016	0.412 $\pm$ 0.011	1.77 $\pm$ 0.07	63
3.1	0.431 $\pm$ 0.017	0.441 $\pm$ 0.012	1.87 $\pm$ 0.07	66

\*From Exp. 8, Table II. The data are also shown in Fig. 4. The uncertainties quoted in this table are the standard errors from a linear regression of  $Re(Z)$  vs.  $Im(Z)$ , and from  $\log(R_{pol})$  vs.  $\log f$ .

*Aplysia* (Fig. 4), assuming various values of  $C_{sh}$  (Table III). The measured  $C_{sh}$  in this experiment was 2.7 pF, which led to the calculated resistivity of 61  $\Omega$ -cm. In all cases the data, after correction for  $C_{sh}$ , could be well fit by Eqs. (2) and (3); the correlation coefficients of the linear regressions of  $Re(Z)$  vs.  $Im(Z)$ , and  $\log(R_{pol})$  vs.  $\log f$  were typically 0.995–0.999. Decreasing  $C_{sh}$  from 2.7 pF to 2.3 pF resulted in a 15% decrease in the calculated value of  $\rho$ , and caused  $\alpha$  (calculated from the phase angle of  $Z_{pol}$ ) to become greater than  $\alpha$  (from the frequency dependence of  $R_{pol}$ ). From Table II we note that these values of  $\alpha$  differ from each other by an average of 11%, suggesting (from Table III), the possibility of a systematic underestimate of the *Aplysia* somatoplasmic resistivity of 15–20%. Alternately, the empirical equations 2 and 3 might not be totally accurate. This systematic error, if present at all, should affect the barnacle results to a lesser extent, because of the relatively lower electrode polarization in these cells. We conclude that the most probable systematic errors in the calculated resistivity of *Aplysia* somatoplasm are within the variance in the data.

Evidently, the high frequency resistivity of *Aplysia* cytoplasm is roughly twice that of the seawater surrounding the cells. Given the relatively large variance of our results and the unknown conductances of the organic anions in this tissue, we cannot meaningfully compare our results to theoretical values of the cytoplasmic resistivity, and so cannot speculate about possible physical mechanisms for this increase in resistivity. However, the high frequency resistivities which we observe are within the range reported in other tissues from marine animals.

In the previous studies using a single metal microelectrode, the magnitude,  $|Z|$ , of the electrode impedance was measured at a frequency (100 KHz) such that electrode polarization effects should dominate the measurements. The present experiments employed much larger electrodes (with correspondingly smaller polarization impedances), and higher frequencies, than the previous work. We have found that the frequency-dependent part of the electrode impedance increases 10-fold after an *Aplysia* neuron (but not a barnacle muscle fiber) is penetrated; its phase angle is unchanged. If this

increase reflected the series impedance of membranes interposed between the micro-electrode and the external ground electrode, we would expect a large change in the phase of the impedance as well as in its magnitude. Evidently, the physical effects which produce a complex electrode impedance in the KCl solutions also determine the electrode impedance when it is inside a cell. A plausible explanation for this impedance increase is that intracellular membranes adhere to the exposed metal tip, decreasing the effective electrode area and correspondingly increasing the total polarization impedance. This would account for the previous measurements at 100 kHz. Paradoxically, this effect apparently does not occur when the electrode penetrates a squid giant axon (11), which also contains many membrane-bound organelles, as shown by electron micrographs (17, 18). This effect needs further study.

An alternate measurement of intracellular impedance employs a linear array of metal microelectrodes (19). Current pulses ( $\Delta I$ ) are passed between the outer two electrodes, and the voltage pulses ( $\Delta V$ ) across the central electrodes measured using a high input impedance amplifier. Although the current pulses contain most of their energy in the audio frequency region (therefore, the electrode polarization impedances are large), the strict proportionality in (19) between the electrolyte resistivity and the transfer impedance of the array,  $\Delta V/\Delta I$ , suggests that the cellular impedance data are probably not affected by electrode polarization artifacts. Since the ionic mobilities in these cells are (from the present study) within a factor of two equal to those in seawater, the intracellular impedance values ( $\sim 400 \Omega$ ) measured using the electrode array almost certainly result from intracellular membranes interposed between the electrodes in these cells. These membranes, of course, determine the effective resistivity of the cell body at the audio frequencies at which the cell normally functions. The earlier work suggests that this low frequency resistivity can be quite high, in spite of high conductivity of the aqueous phase in the cytoplasm.

We thank Dr. Kenneth S. Cole for a number of useful suggestions, and for reviewing an earlier version of this manuscript.

Received for publication 30 April 1976.

## REFERENCES

1. COLE, K. S., and A. L. HODGKIN. 1939. Membrane and protoplasm resistance in the giant squid axon. *J. Gen. Physiol.* **22**:671-687.
2. FALK, G., and P. FATT. 1964. Linear electrical properties of striated muscle fibres observed with intracellular electrodes. *Proc. R. Soc. Lond. B. Biol. Sci.* **160**:69-123.
3. FATT, P., and B. KATZ. 1953. The electrical properties of crustacean muscle fibers. *J. Physiol. (Lond.)* **120**:171-204.
4. KATZ, B. 1948. The electrical properties of muscle fiber membrane. *Proc. R. Soc. Lond. B. Biol. Sci.* **135**:506-534.
5. HODGKIN, A. L., and S. NAKAJIMA. 1972. The effect of diameter on the electrical constants of frog skeletal muscle. *J. Physiol. (Lond.)* **221**:105-120.
6. FATT, P. 1964. An analysis of the transverse electrical impedance of striated muscle. *Proc. R. Soc. Lond. B. Biol. Sci.* **159**:606-651.
7. FRICKE, H., and H. J. CURTIS. 1934. Specific resistance of the interior of the red blood corpuscle. *Nature (Lond.)* **133**:651.

8. CARPENTER, D. O., M. M. HOVEY, and A. F. BAK. 1971. Intracellular conductance of *Aplysia* neurons and squid axon as determined by a new technique. *Int. J. Neurosci.* 2:35-48.
9. CARPENTER, D. O., M. M. HOVEY, and A. F. BAK. 1973. Measurement of intracellular conductivity in *Aplysia* neurons: evidence for organization of water and ions. *Ann. N.Y. Acad. Sci.* 204: 502-533.
10. SCHNEIDER, W. 1975. Theory of the frequency dispersion of electrode polarization. Topology of networks with fractional power frequency dependence. *J. Phys. Chem.* 79:127-136.
11. CARPENTER, D. O., M. M. HOVEY, and A. F. BAK. 1975. Resistivity of axoplasm. II. Internal resistivity of giant axons of squid and *Myxicola*. *J. Gen. Physiol.* 66:139-148.
12. COLE, K. S. 1975. Resistivity of axoplasm. I. Resistivity of extruded squid axoplasm. *J. Gen. Physiol.* 66:133-138.
13. SCHWAN, H. P. 1963. The determination of biological impedances. In *Physical Techniques in Biological Research*. W. L. Nastuk, editor. Academic Press, N.Y. 6:323-407.
14. ROBINSON, D. A. 1968. The electrical properties of metal microelectrodes. *Proc. IEEE.* 56:1065-1071.
15. FRICKE, H. 1932. The theory of electrode polarization. *Phil. Mag.* (7). 14:310-318.
16. PAULY, H., and H. P. SCHWAN. 1966. Dielectric properties and ion mobilities in erythrocytes. *Biophys. J.* 6:621-639.
17. METUZALS, J., and C. S. IZZARD. 1969. Spatial patterns of threadlike elements in the axoplasm of the squid (*Loligo pealii* L.) as disclosed by differential interference microscopy and by electron microscopy. *J. Cell Biol.* 43:456-479.
18. METUZALS, J. 1969. Configuration of a filamentous network in the axoplasm of the squid (*Loligo pealii* L.) giant nerve fiber. *J. Cell Biol.* 43:480-505.
19. HOVEY, M. M., A. F. BAK, and D. O. CARPENTER. 1972. Low internal conductivity of *Aplysia* neuron somata. *Science (Wash., D.C.)* 176:1329-1330.